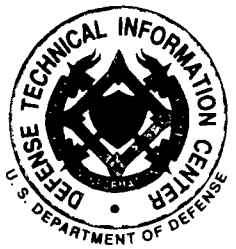

Defense Technical Information Center Compilation Part Notice

This paper is a part of the following report:

• *Title:* Technology Showcase: Integrated Monitoring, Diagnostics and Failure Prevention. Proceedings of a Joint Conference, Mobile, Alabama, April 22-26, 1996.

• *To order the complete compilation report, use:* AD-A325 558

The component part is provided here to allow users access to individually authored sections of proceedings, annals, symposia, etc. However, the component should be considered within the context of the overall compilation report and not as a stand-alone technical report.

WAVELET DOMAIN CHARACTERIZATION & LOCALIZATION OF MODAL ACOUSTIC EMISSIONS IN AIRCRAFT ALUMINUM

Grant A. Gordon, PhD and Randy K. Young, PhD
The Pennsylvania State University
Applied Research Laboratory
PO Box 30
State College, PA 16804 USA
gag100@psu.edu

Abstract: As machines age, broadband acoustic emission (AE) signals are emitted from unknown locations, often due to microscopic material degradation. Not only is the AE source location unknown, but the source mechanism and hence signal characteristics are also unknown. These signals then propagate along multiple, complex geometric paths, in various distorting modes experience mode conversion and wave guide selection, before finally reaching the sensors. In addition to this wave distortion, the signals are corrupted by the noisy and interference-rich environment. If we wish to improve our understanding about the "health" or state of a mechanical system, we should employ AE analysis methods which can more effectively account for these physical effects. This paper presents a technique for detecting, classifying and localizing these acoustic emissions. Due to the significant uncertainty surrounding these sensed signals, high fidelity, well verified models are uncommon. Starting from wide-band, high-fidelity AE data we have shown that it is possible to determine source location with greater accuracy than is possible by traditional source location techniques. This improvement was achieved by considering the multimode wave nature of the AE events, and by applying wide band signal processing techniques that specifically accounted for the dispersive nature of the signals.

Key Words: Acoustic emissions; condition based maintenance; Integrated Predictive Diagnostics; multi-modal propagation; wavelet transforms

INTRODUCTION: Heuristically, or perhaps superficially, it is easy to understand the phenomena of acoustic emission and to acknowledge the importance of this phenomena to a condition based maintenance strategy for machinery. After all, acoustic emission is the internal generation of transient elastic waves by the rapid release of energy from a localized source or sources from within a material. The source mechanisms can vary considerably, but are generally associated with a discontinuous, irreversible, microscopic event. Given this description, one would expect that cracks produced in a material from loading or environmental attack during

service, could be ideally studied via acoustic emission. It is not difficult to imagine that a network of permanent sensors could permit continuous monitoring of defect growth. Used in concert with fracture mechanics principles, a crack growth rate could be measured and the remaining life before the crack reached a critical size determined. Indeed, there has been considerable research in this area, with typical early work [1-3] beginning in the mid 1970's. However, this problem has proven to be more difficult to solve than was initially anticipated. Relationship which link relevant damage measures to an acoustic emission parameters rarely work except in very special situations [3, 4]. Furthermore, the use of AE parameters to identify imminent failure has been even less successful.

Historically AE technology has been primarily concerned with assigning and collecting AE signal 'parameters'. Signal characteristics, such as rise time, peak amplitude, and energy, are evaluated from the filtered response of a resonant transducer used to sense the transient signals. The parameters are evaluated by mathematically describing the sensed waveform as a damped sinusoid. This procedure, which originally appeared warranted when AE was in its infancy due to hardware limitations, is predicated on the assumption that the essential acoustic emission features can be well represented with the single model structure for the data. Unfortunately there is no theoretical basis to support this contention [5], and although researchers have tried to find meaningful correlations between these simple parameters and physically relevant values, the results have not been compelling. For example, the literature is full of conflicting results over the significance of AE amplitudes and source mechanisms [6]. The purpose of the waveform parameterization is to reduce the AE events to their essential characteristics, however many claim that just the opposite occurs. Instead of preserving information, the resonant transducer sensing, nonlinear filtering and amplification, followed by simplistic waveform modeling, actually destroys much of the true information that can be extracted from an AE signal.

Recently a new approach to practical field-based acoustic emission has been proposed [5], and is being pursued [6-9], since it holds considerable promise in being able to extend the limitations of traditional AE. In contrast with the traditional technique, the new approach places emphasis on recording the entire acoustic emission event with as much fidelity and bandwidth as possible. This distinction is significant. By accurately recording the entire waveform, wave propagation theory can be employed for superior source identification and determination of source location. This greatly enhances the ability to distinguish noise from relevant AE signals; a particularly vexing issue in practical monitoring situations. The purpose of this paper is to demonstrate how wide band signal processing techniques, along with wave propagation theory can be used to exploit this rich data set and improve the acoustic emission source identification and location.

ACOUSTIC EMISSION IN PLATES: In acoustic emission the structure being studied is often geometrically platelike; the structure's thickness is much smaller than its length or width. An ideal approximation to these structure is the infinite plate waveguide with traction free boundary conditions. Through a process of multiple reflection, the boundaries of a waveguide actually act to guide the wave energy along the direction of the constraining structure. In this manner the wave modes supported within the guide can follow curvatures, provided the radius of curvature is much larger than the wavelength. This situation is encountered in many aircraft fatigue crack problems, where AE systems are being developed to monitor in-flight crack growth. Cracks are

initiated at fatigue critical regions such as the point where fasteners are used to bond the aircraft skin (platelike) to underlying ribs, spars and/or other plates. When the crack progresses, AE energy is released and guided wave modes are generated which travel through the skin material.

The solution to the problem of elastic wave propagation in an isotropic solid plate, with traction free boundary conditions, has been know for many years. There are three distinct types of guided waves, horizontally polarized shear waves, longitudinal (also known as extensional) plate waves with displacements symmetric about the plate center line and flexural plate waves having antisymmetric displacements. For each of these wave types many possible modes can exist, the solution of which is dictated by a transverse resonance principle. Only those combinations of frequency and phase velocities which generate standing waves in the thickness direction will exist. By mapping out this relationship between frequency and phase velocity a set of dispersion curves can be obtained which prescribes the speed at which a particular frequency component of a transient wave packet will travel if its mode is known.

Often simplifications can be made. In has been observed experimentally [5, 6, 9] that acoustic emission signals in thin plates propagate primarily in the lowest order symmetric (S_0) and antisymmetric (A_0) Lamb wave modes. The dispersion relations for these extensional and flexural plate wave modes are given by the Rayleigh-Lamb equation [10]. For the symmetric modes,

$$\frac{\tan\left(\beta\frac{d}{2}\right)}{\tan\left(\alpha\frac{d}{2}\right)} = -\frac{4\alpha\beta k^2}{\left(k^2-\beta^2\right)^2} \tag{1}$$

and for the antisymmetric modes,

$$\frac{\tan\left(\beta\frac{d}{2}\right)}{\tan\left(\alpha\frac{d}{2}\right)} = -\frac{\left(k^2-\beta^2\right)^2}{4\alpha\beta k^2} \tag{2}$$

where

$$\alpha^2 = \frac{\omega^2}{C_L^2} - k^2 \tag{3}$$

$$\beta^2 = \frac{\omega^2}{C_T^2} - k^2 \tag{4}$$

d is the plate thickness, k is the wavenumber, w = 2pf is the angular frequency, C_L is the bulk longitudinal wave velocity, and C_T is the bulk shear wave velocity. Given a particular isotropic plate material of known thickness, C_T, C_L and d are defined. Using these values equations (1) to (4) can be numerically solved for the two unknowns w and k. This then can be used to determine the phase velocity

$$c = \frac{\omega}{k} \tag{5}$$

which is usually plotted against the dimensionless abscissa variable fd. All modes, other than the two fundamental modes, S_0 and A_0, exhibit cut off frequencies above zero frequency, f = 0.

These cut off frequencies can be determined by forcing k to approach 0 in (1) - (4), which allows us to determine that the next closest mode is the second antisymmetric mode (A_1) with a cut off frequency of $f=C_T/2d$.

Although these dispersion equation appear straight forward, they are quite ill-behaved and present a number of difficulties even for numerical analysis. As an alternative to this exact description for the dispersion curves, a number of authors [5-7, 9] have been studying high fidelity wide-band AE data using approximate plate theories to describe the wave propagation behavior of the fundamental modes. These solutions

$$C_{ext} = \left[\frac{E}{(1-\upsilon^2)\rho}\right]^{\frac{1}{2}} \tag{6}$$

$$C_{flex} = \left[\frac{D}{d\rho}\right]^{\frac{1}{4}} \omega^{\frac{1}{2}} \tag{7}$$

where

$$D = \frac{Ed^3}{12(1-\upsilon^2)} \tag{8}$$

E is Young's modulus, r is density, and n is Poisson's ratio, yield much simpler dispersion relationships, but they only apply to the fundamental modes, and are only accurate when the wavelength is much larger than the plate thickness.

Using the value given in Table 1 for 7075 - T6 aluminum, the dispersion curves for the lowest order symmetric (S_0) and antisymmetric (A_0) Lamb wave modes are plotted in Figure 1. Classical plate theory predicts that the S_0 mode is dispersionless while the A0 mode is highly dispersive. This dispersion makes the A_0 mode data more difficult to handle and it is often argued in traditional AE analysis that the flexural wave should be filtered and removed in order to facilitate accurate source location. Unfortunately the existence of a strong extensional mode is not guaranteed since the source itself dictates the nature of the AE emission generation. Figure 1 also shows the Rayleigh-Lamb dispersion calculations which are exact for homogeneous isotropic material. It can be seen that the lowest order modes approach the Rayleigh wave velocity asymptotically as the fd product grows large. Notice also, that the classsical estimates of the wave mode velocities are only accurate when the frequency thickness, fd, product is small. Calculating the cut off frequency of the next "nearest" mode (A1 mode) we find that no higher order modes can exist below a fd product of 1.6 MHz*mm. Thus we can conclude that the classical theory estimates can lose accuracy at fd values which are smaller than those required for admission of higher order modes. In other words, although classical plate theories are not expected to accurately predict the fundamental Lamb wave modes phase velocity response at high fd values, they can also be inaccurate for values of fd which preclude the existence of other higher order modes.

ACOUSTIC EMISSIONS FROM AIRCRAFT WING SPAR: Acoustic emission data was collected on an experimental test bed designed to simulate a section of an aircraft lower wing. The single layer skin material, 3.175mm 7075-T6 aluminum, was attached to frame members through bolt fasteners at the locations shown in Figure 2. A starter notch to seed crack growth was generated at the midpoint between the rows of fasteners via an access hole. When loading was applied, any AE signals that exceeded a preset threshold level, triggered the simultaneously storage of the AE signals at each of the four sensor locations surrounding the starter notch. The coordinates, in inches, of these transducers and the notch are also shown in Figure 2. A new measurement system called the Fracture Wave Detector manufactured by Digital Wave Corporation, Englewood, Colorado was used to monitor, amplify and store the data recorded by the transducers. This multi-channel transient capture system digitized each transducer responses at a rate of 12.5 MHz for a total record length of 1024 bytes per waveform.

ACOUSTIC EMISSION DATA AND COMPARATIVE ANALYSES: Typical examples of data collected during the experiment, labeled event #1 through #4 for convenience, are shown in Figure 3. Each event shows the simultaneously collected response of the four transducer located at the positions indicated in Figure 2. The data shown in events 1 and 2 are indicative of cracking while the data from events 3 and 4 are generated from noise. This determination is made by considering such factors as frequency content, temporal relationship between the four responses, the duration, amplitude and shape of the signals. For our purposes noise will be considered as any AE signal that arises from a source other than the crack growth mechanism. This can be due to testing machine noise, grip induced damage, electro-magnetic interference, rubbing and mechanical sources. Since cracking is associated with the rapid release of energy we expect the time duration to be short. In carefully controlled ideal experiments [e.g. 9], the two lowest order plate wave modes were identified and their frequency content observed to be different. The flexural waves exhibit more low frequency content than the extensional waves, and because of this, suffer less attenuation as they travel along the plate since attenuation increases as the square of frequency. These waves also shows considerably greater spreading in the time domain due their highly dispersive nature; the lower frequencies lag the faster high frequency components. These shape and frequency features can be used to discriminate between noise and crack signals. In addition, from the sensor location, we can determine the path length difference between the anticipated AE source and the various receivers. This can be used to quantify the expected offset time between the four records, and to further screen out spurious events.

Table 1. Properties of a 7075-T6 aluminum plate.

Young's Modulus	Poisson's Ration	Density	Longitudinal wave velocity	Shear wave velocity	Thickness
71 GPa	0.30	2700 kg/m^3	5950 mm/us	3180 mm/us	3.175 mm

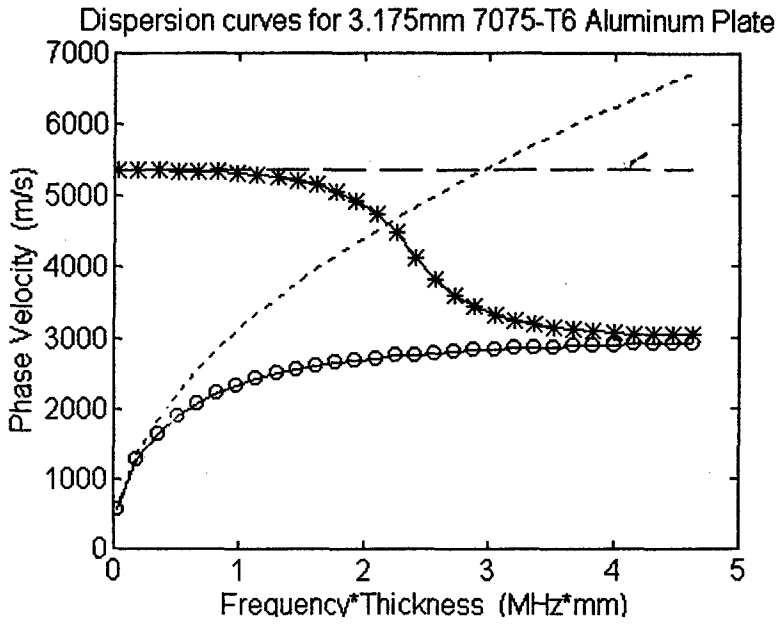

Figure 1. Dispersion curves for the S_0 and A_0 modes in 3.175mm thick 7075 - T6 aluminum plate. The dashed and dotted lines are for the S_0 and A_0 modes respectively, calculated using classical plate theory. The solid line with stars and the solid line with circles are for the S_0 and A_0 modes respectively, calculated using the transcendental Rayleigh-Lamb equations.

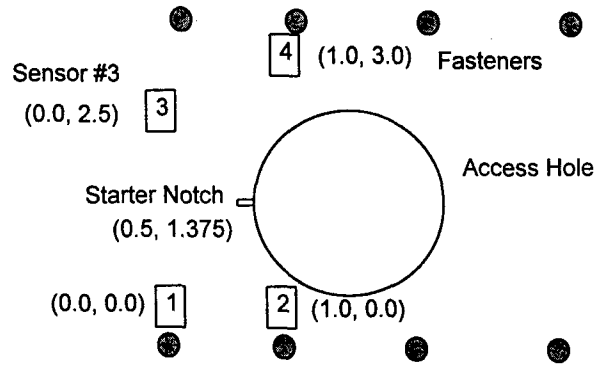

Figure 2. Experimental setup showing sensor location and notch geometry.

Many of these wave mode features can be observed in the power spectra and spectrogram plots of our data. In Figure 4 the power spectra of two typical AE signal are compared. The top half of the figure shows the power spectrum of an AE crack signal. This plot shows a significant amount of energy both above and below 1 MHz. The energy above 1 MHz is probably due to the S_0 mode. However, we can not rule out the possibility that this contribution is due to higher order modes, since its fd product exceeds the A1 mode cut off limit. Notice that the amplitude of the high frequency content is smaller than the lower frequency content due to the flexural wave. The noise signal shown in the bottom half of the figure has much lower frequency content. Figure 5 shows how the frequency content of a typical crack signal varies with time. Lighter areas indicate higher energy concentration. Again we see two main area of frequency content; a strong concentration below 1 MHz and a weaker concentration above 1 MHz. Initially these 'packets' arrive at the sensor at roughly the same time, as shown by the two lightest areas of the spectrogram. However as time progresses, the low frequency content dominates. This is consistent with our model of a multimode signal comprised of a weak extensional mode and a strong flexural mode. The fact that the low frequency components of the A_0 mode lag the faster high frequency components is also seen in the spectrogram.

To further analyze the data we will consider the problem of source location. Since the source location is assumed to be known, the accuracy of the location estimate will be used to evaluate the effectiveness of various processing approaches. Let (x_0 , y_0) be the position of the source, which is to be estimated. For each sensor located at a unique (x_i , y_i) the following relation will be satisfied

$$(x_0 - x_i)^2 + (y_0 - y_i)^2 = (ct_i)^2 \tag{9}$$

when a signal is sensed; ti is the time for the wave to reach the sensor and c is the wave velocity. Since only the time differences between the sensors can be measured from the data, we substitute $t_i = t_0 + \Delta t_i$, where t_0 is the time required for the wave to reach the closest sensors. By substituting each of the four sensors into equation (9) and subtracting any ith sensor expression from a jth sensor expression, we produce a set of six linear equation. From this overdetermined set of equations, the three unknowns (x_0, y_0, t_0) can be found given the wave speed, time differences and sensor location, by the method of least squares.

Traditionally the time of flight differences between sensors is determined using threshold triggering. The time difference is measured from the first occurrence at which the sensed signal rises above a threshold level on each sensor. Since the extensional wave travels faster than the flexural wave it is customary to assume that this wave mode is responsible for the threshold triggering and to assign an extensional wave velocity (equation (6)) for use in the location algorithm. As already pointed out, the type of wave mode generated is dependent of the AE source. In-plane cracking yields higher extensional mode amplitudes, while source mechanisms that produce displacement perpendicular to the plane give rise to flexural modes. Clearly it is not always accurate to assume that the extensional mode contributions are significant enough to rise above the threshold level. In our data we have determined that contributions from the antisymmetric mode dominate, especially at low frequencies. To make use of this data we used a

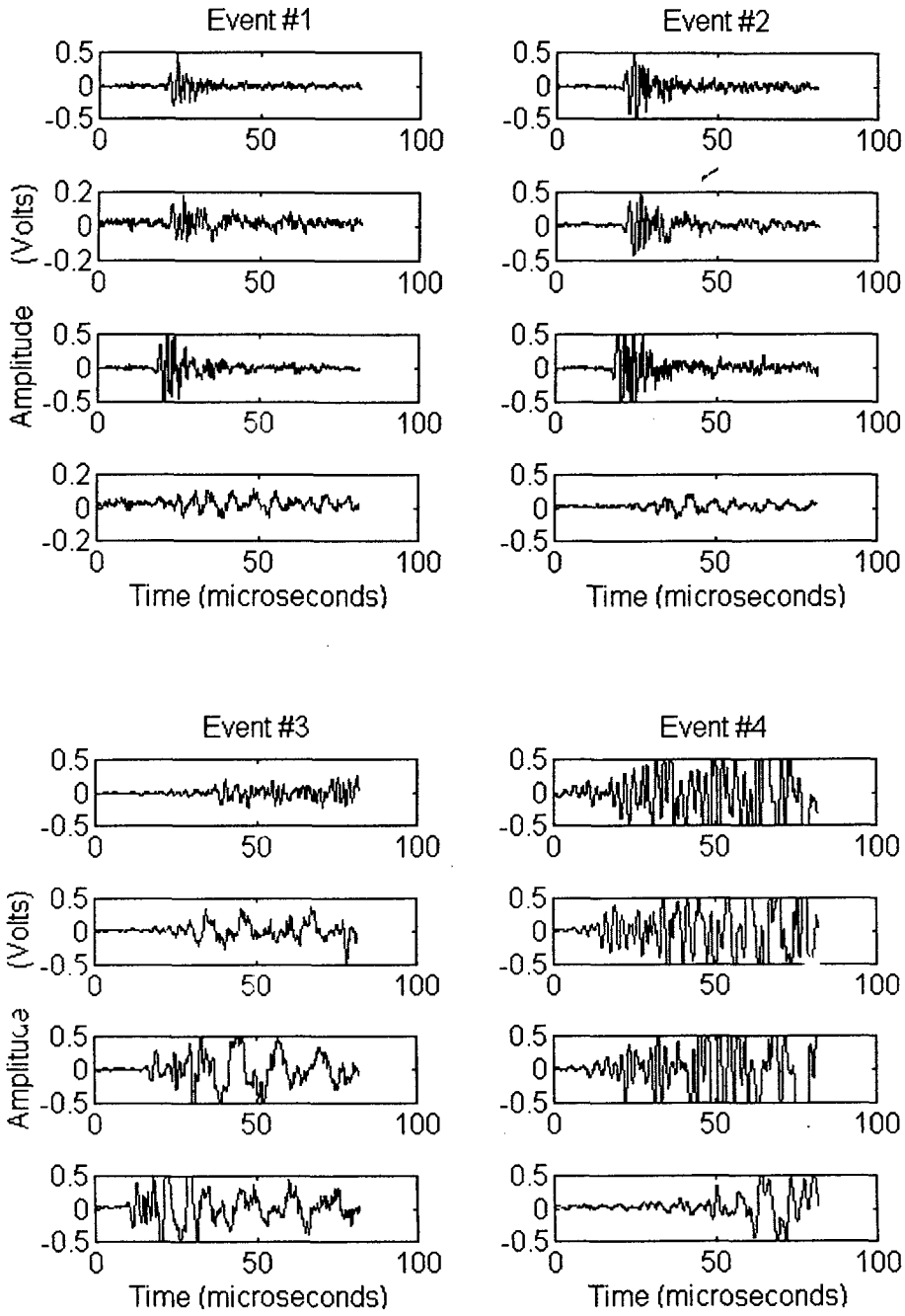

Figure 3. Sample acoustic emission data. All four transducer responses for an AE event are given in a single column, ordered from top to bottom to correspond with the responses of the first through fourth transducer.

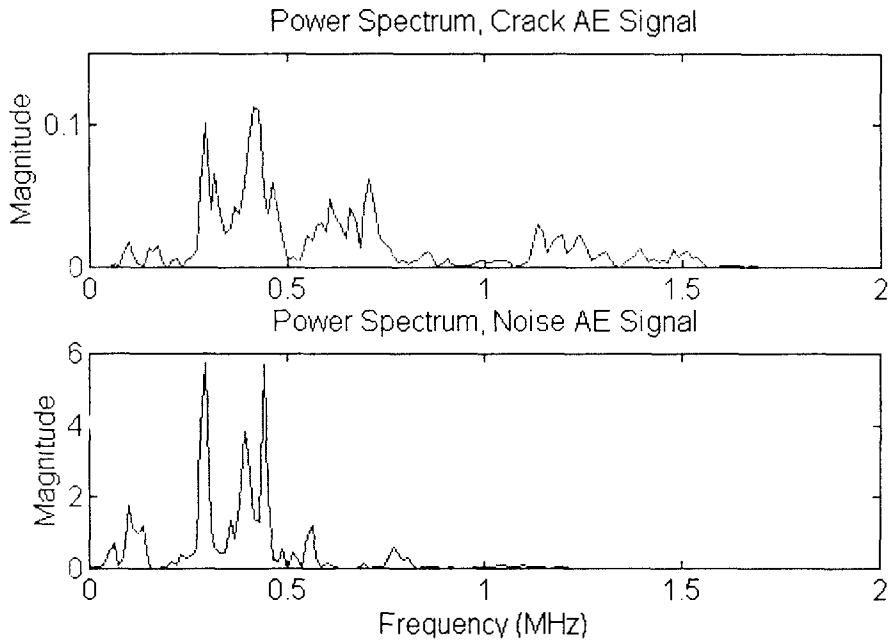

Figure 4. Typical power spectral density curves for the crack and noise data.

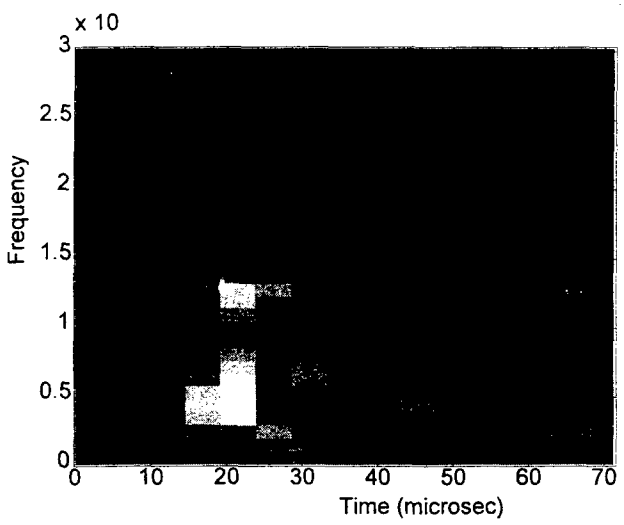

Figure 5. Typical spectrogram for the crack AE signals showing the distribution of frequency with time.

novel approach based on wide band processing. The method can be considered a time domain spectroscopy (TDS) technique where the sampled signals are processed by a bank of the narrowband filters defined by the Morlet wavelet

$$\Psi(t) = \exp(j\omega t)\exp\left(-\frac{t^2}{2}\right) \tag{10}$$

This is nothing more than a complex sinusoid windowed modulated by a Gaussian envelope where the frequency to be extracted from the data is used to define the center frequency of the wavelet. Subsequent filtering of the wide band signals is performed by multiplication of the Fourier transformed filter response by the spectral response of each sensor record. By performing this operation repetitively, at various prescribed frequencies, we built up a filter bank decomposition of the data. The time difference between sensors was found, for each filtered component of the data, by performing the inverse Fourier transform and cross correlating the resulting waveforms. Cross correlation will show a peak at the corresponding time lag position which is equal to the delay between the two signals. Since the wide band data has been filtered into narrowband responses the cross correlated time differences can be taken as phase delays. To determine the source location from these new narrowband time differences, equations (2)-(4) were used to define the appropriate phase velocity. This mechanism provide a rich set of location estimates that could be averaged to yield a robust estimate of the crack source location.

Table 2. Comparison of AE source location estimates

Data	Threshold Value	Location Estimate	Error	Data	Frequency (KHz)	Location Estimate	Error
Event #1	.1	(.666, 1.00)	.406	Event #1	600	(.317, 1.32)	.190
	.05	(-.071, -5.62)	1.24		500	(.437, 1.37)	.063
					400	(.570, 1.26)	.130
					300	(.534, 1.26)	.110
				average	n/a	(.465, 1.30)	.082
Event #2	.1	(.671, 1.01)	.403	Event #2	600	(.419, 1.32)	.100
	.05	(1.95, 1.57)	1.46		500	(.470, 1.27)	.109
					400	(.377, 1.28)	.151
					300	(.441, 1.31)	.110
				average	n/a	(.427, 1.29)	.112
Event #3	.1	(-3.47, -2.73)	5.72	Event #3	600	(.613, .735)	.650
	.05	(-3.09, -.795)	4.19		500	(.119, -.336)	1.75
					400	(.985, 1.89)	.710
					300	(.226, 2.55)	1.20
Event #4	.1	(1.70, 1.71)	1.24	Event #4	600	(.603,1.27)	.144
	.05	(6.16, -4.79)	8.37		500	(.195,1.19)	.356
					400	(.517, 1.24)	.129
					300	(.301, 1.27)	.223

The left hand side of Table 2 shows the results of using the traditional thresholding approach to AE source location. An S_0 wave velocity of 5375 mm/ms was used in the calculation and the error was determined by finding the distance of the estimate from the assumed AE crack source location at the starter notch. Table 2 also shows the results of the new time domain spectroscopy approach for determining AE source location. Four frequency values, centered around the low frequency spectral content of the AE signals (Figure 4) are shown. It can be seen that this approach gives a much better estimate of the source location, especially when the various estimates are combined via averaging. From both techniques we can see that the location of AE events #3 was placed far from the crack site. This further confirms our assessment that this signal was not due to a cracking event. Event #4 is also placed far from the crack site by the thresholding technique, but not by the spectroscopy technique. We believe that this event is also due to noise but that the spectroscopy technique experienced difficulty because of the strongly clipped nature of the signal, Figure 3.

CONCLUSIONS: Starting from wide-band high-fidelity AE data we have shown that it is possible to determine source location with greater accuracy than is possible by traditional source location techniques. This improvement was achieved by considering the multimode wave nature of the AE events and by applying wide band signal processing techniques that specifically accounted for the dispersive nature of the signals.

ACKNOWLEDGMENTS: The authors would like to thank Paul Lacjak and Michael Gorman of Digital Wave Corporation for providing the data and for illuminating discussions.

REFERENCES:

[1] Harris, P.H. and Dunegan, H.L. "Continuous monitoring of fatigue-crack growth by AE techniques," Expl Mechs, **14**, Feb. 1974, pg 71.
[2] Tetelman, A.S. and Evans, A.G. "Failure prediction in brittle materials using fracture emchanics ans AE," UCLA-ENG-7365, Aug. 1973.
[3] Williams, J.H, DeLonga, D.M., and Lee, S.S. " Correlations of AE with fracture mechanics parameters instructural bridge steels during fatigue," Materials Evaluation, **40**, p1184, 1982.
[4] Scott, I.G. Basic Acoustic Emission, Gordon and Breach Science Publishers, NY, NY, 1991.
[5] Gorman, M.R., "New Technology for Wave Based Acoustic Emission and Acousto-Ultrasonics," pp. 47-59 in AMD-vol **188**, Wave Propagation and Emerging Technologies, ASME, NY, NY, 1994
[6] Prosser, W.H., Jackson, K.E., Kellas, S., Smith, B.T., McKeon, J., and Friedman, A. "Adavnced waveform-based acoustic emission detection of matrix cracking in composites," Material Evaluation, **53**, Sept 1995, p1082.
[7] Searle, I., Ziola, S., and Rutherford, P. "Crack detection in lap-joints using acoustic emission," SPIE, **2444**, p212.
[8] Martin, C.A., Van Way, C.B., Lockyer, A.J., Kudva, J.N., and Ziola, S. "Acoustic emission testing on an F/A - 18 E/F Titanium bulkhead," SPIE, **2444**, p204.
[9] Gorman, M.R. "Plate Wave Acoustic Emission," pp. 358-364, JASA, **90**, No. 1, 1991.
[10] Graff , K. Wave motion in elastic solids, Dover Pub., Inc., NY NY, 1975.

//